

# Jet and hadron production in photon-photon collisions\*

Stefan Söldner-Rembold <sup>a</sup> \*

<sup>a</sup> Universität Freiburg, Hermann-Herder-Str.3, D-79104 Freiburg im Breisgau, Germany

Di-jet and inclusive charged hadron production cross-sections measured in  $\gamma\gamma$  collisions by OPAL are compared to NLO pQCD calculations. Jet shapes measured in  $\gamma\gamma$  scattering by OPAL, in deep-inelastic ep scattering by H1 and in  $\gamma p$  scattering by ZEUS are shown to be consistent in similar kinematic ranges. New results from TOPAZ on prompt photon production in  $\gamma\gamma$  interactions are presented.

## 1. Leading Order parton processes

The interaction of quasi-real photons ( $Q^2 \approx 0$ ) studied at LEP and the interaction of a quasi-real photon with a proton studied at HERA (photo-production) are very similar processes. In leading order (LO) different event classes can be defined in  $\gamma\gamma$  and  $\gamma p$  interactions. The photons can either interact as ‘bare’ photons (“direct”) or as

hadronic fluctuations (“resolved”). Direct and resolved interactions can be separated by measuring the fraction  $x_\gamma$  of the photon’s momentum participating in the hard interaction for the two photons. In  $\gamma\gamma$  interactions they are labelled  $x_\gamma^\pm$  for the two photons.

Ideally, the direct  $\gamma\gamma$  events with two bare photons are expected to have  $x_\gamma^+ = 1$  and  $x_\gamma^- = 1$ , whereas for double-resolved events both values  $x_\gamma^+$  and  $x_\gamma^-$  are expected to be much smaller than one. In photoproduction, the interaction of a bare photon with the proton is labelled ‘direct’ (corresponding to ‘single-resolved’ in  $\gamma\gamma$ ) and the interaction of a hadronic photon is called ‘resolved’ (corresponding to ‘double-resolved’ in  $\gamma\gamma$ ).

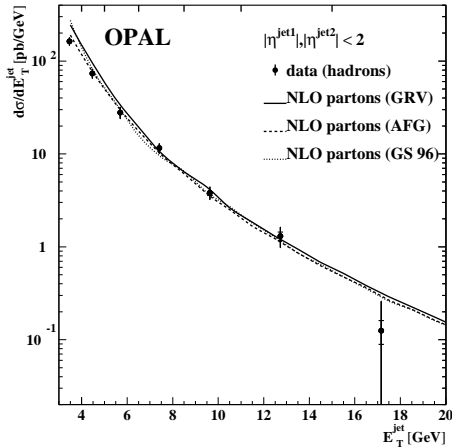


Figure 1. The inclusive  $e^+e^-$  di-jet cross-section as a function of  $E_T^{\text{jet}}$  for jets with  $|\eta^{\text{jet}}| < 2$ .

## 2. Di-jet production

Studying jets gives access to the parton dynamics of  $\gamma\gamma$  interactions. OPAL has therefore measured di-jet production in  $\gamma\gamma$  scattering at  $\sqrt{s_{ee}} = 161 - 172$  GeV using the cone jet finding algorithm with  $R = 1$  [ 1].

The differential cross-section  $d\sigma/dE_T^{\text{jet}}$  for di-jet events with pseudorapidities  $|\eta^{\text{jet}}| < 2$  is shown in Fig. 1. The measurements are compared to a parton level NLO calculation [ 2] for three different NLO parametrizations of the parton distributions of the photon GRV-HO [ 3], AFG [ 4] and GS [ 5]. The calculations using the three different NLO parametrizations are in good agreement with the data points except in the first bin where theoretical and experimental uncertainties

\*Heisenberg-Fellow

\* submitted to the proceedings of DIS99, DESY-Zeuthen, Berlin, Germany, April 1999

are large.

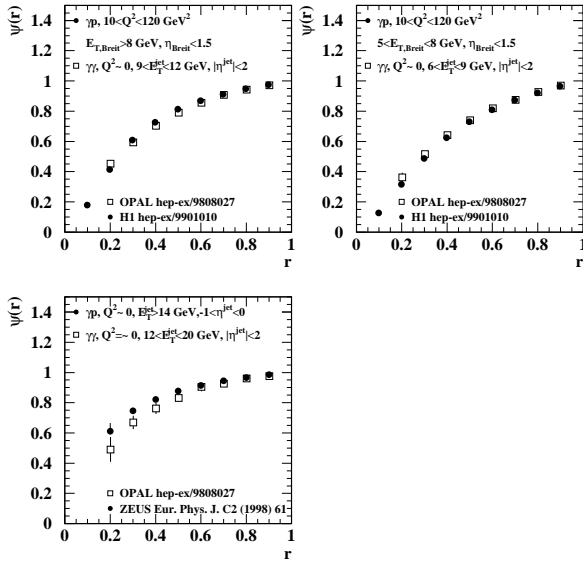


Figure 2. A comparison of jet shapes  $\psi(r)$  measured in di-jet events by OPAL, H1 and ZEUS.

### 3. Jet shapes

The jet shape is characterised by the fraction of a jet's transverse energy ( $E_T^{\text{jet}}$ ) that lies inside an inner cone of radius  $r$  concentric with the jet defining cone:

$$\psi(r) = \frac{1}{N_{\text{jet}}} \sum_{\text{jets}} \frac{E_T(r)}{E_T(r=R)}, \quad (1)$$

where  $E_T(r)$  is the transverse energy within the inner cone of radius  $r$  and  $N_{\text{jet}}$  is the total number of jets in the sample. The jet shapes are corrected to the hadron level using the Monte Carlo. It has been shown by OPAL that the jets become narrower with increasing  $E_T^{\text{jet}}$ , that the jet shapes are nearly independent of  $\eta^{\text{jet}}$  and that gluon jets are broader than quark jets [ 1].

The measured jet shapes are compared to data from the HERA experiments in similar kinematic ranges. H1 has measured jet shapes for di-jet events produced in deep-inelastic scattering (DIS) with  $10 < Q^2 < 120 \text{ GeV}^2$  and  $2 \cdot 10^{-4} < x < 8 \cdot 10^{-3}$  [ 6]. The events are boosted into the Breit-frame. ZEUS has measured jet shapes in di-jet photoproduction for quasi-real photons in the lab frame [ 7]. In the regions  $\eta_{\text{Breit}} < 1.5$  (H1 data) and  $-1 < \eta^{\text{jet}} < 0$  (ZEUS data), most jets should be quark jets. The same is true for the OPAL data at relatively large  $E_T^{\text{jet}}$ , where the direct process dominates. A comparison shown in Fig. 2 performed for similar transverse energy ranges shows good agreement of the OPAL  $\gamma\gamma$  and the H1 DIS data. The jets in photoproduction events measured by ZEUS are narrower than the  $\gamma\gamma$  jets. This could be due to the slightly larger  $E_T^{\text{jet}}$  in the ZEUS data. A detailed comparison of jet widths measured in  $\gamma\gamma$  interactions and other processes ( $e^+e^-$ ,  $\bar{p}p$ ,  $\gamma p$ ) has recently been published by TOPAZ [ 8].

### 4. Charged hadron production

Hadron production at large transverse momenta is also sensitive to the partonic structure of the interactions without the theoretical and experimental problem related to the various jet algorithms. Interesting comparisons of  $\gamma\gamma$  and  $\gamma p$  data taken at LEP and HERA, respectively, should be possible in the future, since similar hadronic centre-of-mass energies  $W$  of the order 100 GeV are accessible for both type of experiments.

The distributions of the transverse momentum  $p_T$  of hadrons produced in  $\gamma\gamma$  interactions are expected to be harder than in  $\gamma p$  or hadron- $p$  interactions due to the direct component. This is demonstrated in Fig. 3 by comparing  $d\sigma/dp_T$  for charged hadrons measured in  $\gamma\gamma$  interactions by OPAL [ 9] to the  $p_T$  distribution measured in  $\gamma p$  and  $hp$  ( $h = \pi, K$ ) interactions by WA69 [ 10]. The WA69 data are normalised to the  $\gamma\gamma$  data in the low  $p_T$  region at  $p_T \approx 200 \text{ MeV}/c$  using the same factor for the  $hp$  and the  $\gamma p$  data. The hadronic invariant mass of the WA69 data is about  $W = 16 \text{ GeV}$  which is of similar size

as the average  $\langle W \rangle$  of the  $\gamma\gamma$  data in the range  $10 < W < 30$  GeV.

Whereas only a small increase is observed in the  $\gamma p$  data compared to the  $h\pi$  data at large  $p_T$ , there is a significant increase of the relative rate in the range  $p_T > 2$  GeV/c for  $\gamma\gamma$  interactions due to the direct process.

The  $\gamma\gamma$  data are also compared to a ZEUS measurement of charged particle production in  $\gamma p$  events with a diffractively dissociated photon at  $\langle W \rangle = 180$  GeV [11]. The invariant mass relevant for this comparison should be the mass  $M_X$  of the dissociated system (the invariant mass of the

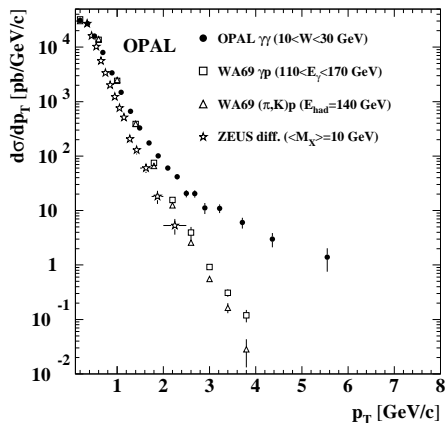


Figure 3. The  $p_T$  distribution measured in  $\gamma\gamma$  interactions in the range  $10 < W < 30$  GeV is compared to the  $p_T$  distribution measured in  $\gamma p$  and  $h p$  ( $h = \pi, K$ ) interactions by WA69 [10]. The cross-section values on the ordinate are only valid for the OPAL data.

‘ $\gamma$ -Pomeron’ system). The average  $\langle M_X \rangle$  equals 10 GeV for the data shown. The  $p_T$  distribution falls exponentially, similar to the  $\gamma p$  and hadron- $p$  data, and shows no flattening at high  $p_T$  due to a possible hard component of the Pomeron.

NLO calculations [12] of the cross-sections  $d\sigma/dp_T$  are shown in Fig. 4. The cross-sections

are calculated using the QCD partonic cross-sections, the NLO GRV parametrisation of the parton distribution functions [3] and fragmentation functions fitted to  $e^+e^-$  data. The renormalisation and factorisation scales are set equal to  $p_T$ . The change in slope around  $p_T = 3$  GeV/c in the NLO calculation is due to the charm threshold. The agreement between the data and the NLO calculation is good.

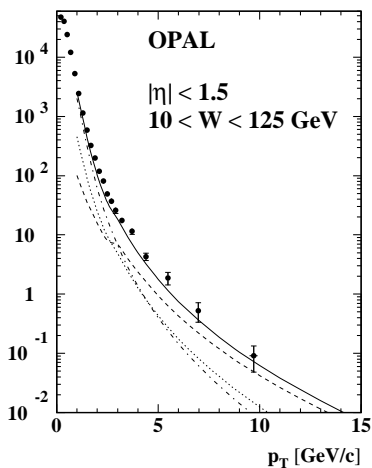


Figure 4.  $d\sigma/dp_T$  for pseudorapidities  $|\eta| < 1.5$  in the range  $10 < W < 125$  GeV compared to NLO calculations for  $p_T > 1$  GeV/c (continuous curve) together with the double-resolved (dot-dashed), single-resolved (dotted) and direct contributions (dashed).

## 5. Prompt photons

The production of prompt photons in  $\gamma\gamma$  interactions can also be used to measure the quark and gluon content of the photon [13]. At TRISTAN energies the single-resolved process  $\gamma q \rightarrow \gamma q$  is expected to dominate the prompt photon production cross-section, whereas at LEP2 energies

double-resolved processes should become important.

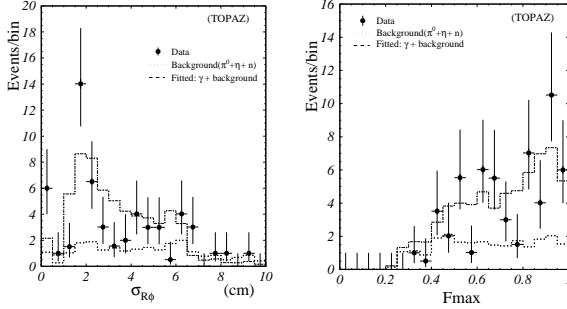


Figure 5. Shower shape parameters,  $\sigma_{R\phi}$  and  $F_{\max}$ , for the prompt photon events measured by TOPAZ.

TOPAZ has measured the prompt photon cross-section  $\sigma(e^+e^- \rightarrow e^+e^-\gamma X)$  by fitting signal plus background (mainly from  $\pi^0$  decays) to variables describing the shower shape in the calorimeter (Fig. 5). The variables are the rms of the cluster width in the  $r\phi$  direction,  $\sigma_{R\phi}$ , and the ratio of the maximum energy in a cluster to the total cluster energy,  $F_{\max}$ .

TOPAZ obtains  $\sigma(e^+e^- \rightarrow e^+e^-\gamma X) = (1.48 \pm 0.4 \pm 0.49)$  pb for photons with energies greater than 2 GeV using a data set with an integrated luminosity of  $L = 288$  pb. This result is about 1.5-2 standard deviations larger than the LO cross-sections  $\sigma(e^+e^- \rightarrow e^+e^-\gamma X)$  of 0.35 pb and 0.50 pb which were obtained with PYTHIA using SaS-1D [14] and LAC1 [15], respectively.

### Acknowledgements

I want to thank Hisaki Hayashii for helping me with the TOPAZ data, Michael Klasen for providing the NLO calculations of the di-jet cross-sections, Tancredi Carli for discussion on the jet shapes and the organizers for this interesting and enjoyable workshop.

### REFERENCES

1. OPAL Coll., hep-ex/9808027, accepted by Eur. Phys. J.
2. M. Klasen et al., Eur. Phys. J. direct C1 (1998) 1, M. Klasen, private communications.
3. M. Glück et al., Phys. Rev. D46 (1992) 1973; Phys. Rev. D45 (1992) 3986.
4. P. Aurenche et al., Z. Phys. C64 (1994) 621.
5. L.E. Gordon and J.K. Storrow, Nucl. Phys. B489 (1997) 405.
6. H1 Coll., C. Adloff et al., Nucl. Phys. B545 (1999) 3; P.-O. Meyer, these proceedings.
7. ZEUS Coll., J. Breitweg et al., Eur. Phys. J. C2 (1998) 61.
8. TOPAZ Coll., K. Adachi et al., Phys. Lett. B451 (1999) 256.
9. OPAL Coll., K. Ackerstaff et al., Eur. Phys. J. C6 (1999) 253.
10. R.J. Apsimon et al., Z. Phys. C43 (1989) 63.
11. ZEUS Coll., M. Derrick et al., Z. Phys. C67 (1995) 227.
12. J. Binnewies et al., Phys. Rev. D53 (1996) 6110.
13. M. Drees and R. Godbole, Phys. Lett. B257 (1991) 425; L.E. Gordon and J.K. Storrow, Phys. Lett. B385 (1996) 385.
14. G.A. Schuler and T. Sjöstrand, Z. Phys. C68 (1995) 607.
15. H. Abramowicz et al., Phys. Lett. B269 (1991) 458.